Compressed Sensing Diffusion Tensor Imaging (DTI) with Tensor and Phase Constraints

Y. Li[1], M. Aggarwal[1], J. Zhang[2], and S. Mori[2]

[1]Biomedical Engineering, Johns Hopkins University School of Medicine, Baltimore, MD, United States, [2]Radiology, Johns Hopkins University School of Medicine, Baltimore, MD, United States

Introduction: To accelerate MR imaging, incomplete k space reconstruction techniques use multiple sources of prior knowledge and information redundancies. e.g. the smoothness of phase map in partial Fourier reconstruction and the transform sparsity in compressed sensing. They were designed for achieving a relatively high reconstruction accuracy from a reduced amount of data. In DTI, multiple (>=6) diffusion weighted images (DWIs) are acquired to estimate the six-parameter tensor model. This means that a large amount of data are collected to extract a relatively small amount of information. We propose to add a constraint to the compressed sensing method that measures the error between reconstructed DWIs and their tensor fitted values. Also, a phase constraint derived from the low resolution phase map estimated from fully sampled central part of k space was applied to the reconstruction. Testing result on high field mouse embryo DTI data shows reduction of reconstruction error by adding each of the proposed constraints and the joint improvement is even more significant.

Methods: Typical compressed sensing reconstructions using transform sparsity as proposed in [1] try to find the reconstructed image $\mathbf{m_r}$, that minimizes a cost function of the form: $\mathbf{m_r}=\mathbf{argmin_m}\sum_i \lambda_i \|\Psi_i \mathbf{m}\|_1$, subject to $\|F_u\mathbf{m}-\mathbf{y}\|_2^2<\varepsilon$ (1), where Ψ_i's are the sparsifying transforms, $\mathbf{y}$ is the measured k space data, F_u is the undersampled Fourier transform and ε is a number related to noise level. Here we add a new constraint which is the sum of norms of errors between DWIs and their tensor model predicted values. All DWIs are reconstructed simultaneously. Then the problem becomes: $\{\mathbf{m}_{rj}, j=1,...,J\}=\mathbf{argmin}_{\{\mathbf{m}j,\, j=1,...,J\}}=\sum_i \lambda_i \sum_j \|\Psi_i \mathbf{m}_j\|_1$, subject to $\sum_j \|F_{uj}\mathbf{m}_j-\mathbf{y}_j\|_2^2<\varepsilon_1$ and $\sum_j \|\mathbf{m}_j-\hat{\mathbf{m}}_j\|_2^2<\varepsilon_2$ (2), where $\mathbf{m}_j$'s are the J DWIs, and $\hat{\mathbf{m}}_j=\mathbf{m}_0\exp(-\mathbf{b}_j^T\hat{\mathbf{D}}\mathbf{b}_j)$ (j=1,...,J) are the corresponding tensor model predicted DW values based non-diffusion weighted image $\mathbf{m}_0$ and $\mathbf{m}_j$'s via the estimated tensor $\hat{\mathbf{D}}$ [2]. In a case where no $\mathbf{m}_0$ image is acquired as in our tested dataset, and linear fitting is used for tensor and $\mathbf{m}_0$ estimation, $\hat{\mathbf{m}}_j=\prod_{i=1}^{J}|\mathbf{m}_i|^{\mathbf{C}ji}$, where the matrix $\mathbf{C}$ is determined by $\mathbf{b}$ vectors[3]. ($\mathbf{C}=\mathbf{AA}^+$, $^+$means pseudo inverse. $\mathbf{A}$ is a J by 7 matrix, the ith row of $\mathbf{A}$ is $-[b_{jx}^2, b_{jy}^2, b_{jz}^2, b_{jx}b_{jy}, b_{jx}b_{jz}, b_{jz}b_{jy}, -1]$, where b_{jx}, b_{jy} and b_{jz} are the 3 components of the jth $\mathbf{b}$ vector). $\hat{\mathbf{m}}_j$'s are differentiable functions of $\mathbf{m}_j$'s if $|\mathbf{m}|$ is approximated by $|\mathbf{m}|=\sqrt{\mathbf{m}^*\mathbf{m}+\mu}$, where * means complex conjugate and μ is a small positive number. The constrained optimization problems in Eq.(1) and Eq.(2) can be converted to unconstrained Lagrangian forms [1] and can be solved by conjugate gradient type algorithms. For phase constraint, [4] shows the k space relationship: $\mathbf{y}=\mathbf{y}^H\otimes\Phi$, where $\mathbf{y}^H$ is the Hermitian of k space data $\mathbf{y}$ and Φ is the Fourier transform of complex exponential of the doubled phase map: $\exp(j2\varphi(\mathbf{x}))$. The phase map in our study is approximated by a polynomial. The polynomial function is calculated by fitting the low resolution phase map reconstructed from central part of k space. We propose an iterative reconstruction scheme: Initialization: $\mathbf{m}_0$=0, $\mathbf{y}_0=\mathbf{y}$, estimate Φ from low resolution phase map. for ith iteration: 1) $\mathbf{y}'_i=\mathbf{y}_{i-1}^H\otimes\Phi$, 2) insert measured values: $\mathbf{y}'_i|_{acq}=\mathbf{y}|_{acq}$, 3) $\mathbf{m}'_i=F^{-1}(\mathbf{y}'_i)$, 4) solve Eq.(2) by conjugate gradient with initial value $\mathbf{m}'_i$, get $\mathbf{m}_i$, and $\mathbf{y}_i=F(\mathbf{m}_i)$; Exit if convergence criterion met.

Results: We tested the proposed method on a mouse embryo DTI dataset, which was acquired by a 11.7T Bruker scanner. Sixteen DWIs of different diffusion directions at bvalues 1000 and four DWIs with low bvalues (190) were acquired using 3D GRASE sequence[5]. Resolution: 136(X, readout)x128(Y) x186(Z); voxel size: 0.059x0.059 x0.059mm^3. Full k space data were acquired and DWIs reconstructed from the full k space data were used as the ground truth. For reconstruction from partial k space data, 2D undersample schemes in the Y-Z plane were used at two reduction factors (RF)(2 for 50% sampled and 4 for 25%, see Fig. 1(d)), then the sagittal slices were reconstructed. Sampling patterns were generated using an Gaussian shaped function that origins at the center of k space as sampling probability and with the central 1/16 area fully sampled. In our study, Daubechies4 wavelet and finite difference were used as sparifying transforms. Third order polynomials were used for approximating the phase maps. Normalized root mean square errors (NRMSE) of the reconstructed DWIs and tensor images were used to measure the reconstruction accuracy. Table 1. shows relatively smaller reconstruction errors in DWIs by using both tensor and phase constraints. The reconstruction accuracy can be further improved by combining the two constraints together. Improvements are bigger when reduction factor is bigger. The improvements in calculated diffusion tensor images are relatively smaller than that of DWIs. Fig 2.shows the proposed method (d) provides clearer details than using Eq.(1) (b) and yields smaller errors(c,e).

Discussions and Conclusion: We demonstrated that applying tensor and phase constraints to compressed sensing DTI can improve reconstruction accuracy. While at RF = 2, we find error of calculated tensor is smallest when only the tensor constraint is added, it is due to the constraint is specifically designed for tensor model. The NRMSE values at RF = 2 are smaller than 0.01(SNR>100) which are comparable with the noise level in routine DWIs, that implies compressed sensing DTI could be practical for fast imaging. The impacts of reconstruction errors on post-processing steps such as fiber tracking will be investigated in the future.

RF	2					4				
Method	(1) only	(2) only	(1)+phase	(2)+phase	Imprv.	(1) only	(2) only	(1)+phase	(2)+phase	Imprv.
NRMSE DWI	0.01215	0.009312	0.009239	0.008186	32.35 %	0.03138	0.02430	0.02403	0.01679	46.50%
NRMSE DT	0.01687	0.01460	0.015396	0.01486	12.01 %	0.03259	0.02988	0.02899	0.02640	19.05%

Table 1. Comparison of NRMSE values of different methods. DT: calculated diffusion tensor. Method '(1)' means by method using Eq.(1); '(2)' means the proposed method using Eq.(2); '+phase' means methods with phase constraint step. Imprv. means change in percent between (1) and '(2)+phase' methods. All values are mean values of 10 slices in tested dataset.

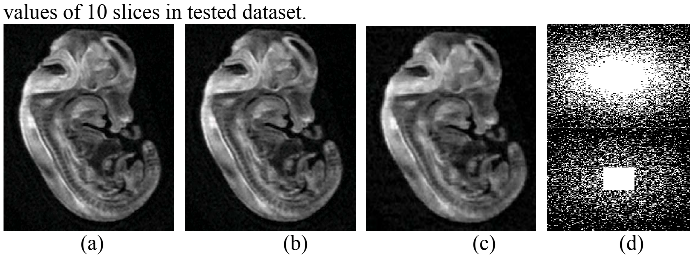

(a) (b) (c) (d)

Fig.1 A slice of DWI: (a) reconstructed from full data (b) reconstructed by proposed method ((2)+phase) with RF = 2 (c), and by proposed method with RF = 4. (d) the sampling patterns for RF = 2(top) and 4(bottom).

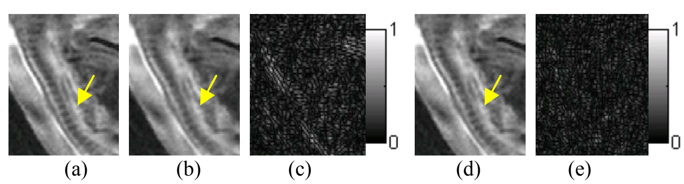

(a) (b) (c) (d) (e)

Fig.2 Enlarged region from the same slice as in Fig.1: (a) reconstructed from full data; (b) reconstructed using Eq.(1) and absolute reconstruction error (c); (d) reconstructed using proposed method '(2)+phase' and absolute error (e). Brightness levels of error images are scaled by the same number for comparison.

Acknowledgement: This study is supported by RO1AG20012 / P41RR15241.

References: [1] Lustig M, Donoho D, Pauly JM. Magnet Reson Med 2007, 58:1182-1195; [2] Basser PJ, Mattielo J, LeBihan D, Biophys J 1994, 66: 259-267; [3] Basser PJ, Mattielo J, Lebihan D, J Magn Reson Ser B 1994, 103:247-254; [4] Huang F, Lin W, Li Y. Magnet Reson Med 2009, 62:1261-1269; [5] Aggarwal M, Mori S, Shimogori T, Blackshaw S, Zhang JY.. Magnet Reson Med 2010, 64:249-261.